

1. Big Bang Nucleosynthesis and the Case of Li, Be, and B

Early in the Big Bang, T so high that electrons, protons, positrons, and neutrons were in thermal equilibrium. The fact that there are baryons today means that initially in the early universe there were more baryons than anti-baryons. All the anti-baryons annihilated with baryons very early, leaving the excess baryons we see today. The ratio of baryons to photons, denoted η_b , does not change with time as both numerator and denominator decline with $a(t)^{-3}$. Since n_γ can be calculated from the CMB radiation we see today, η_b can also be measured.

After the annihilation was over, with $T \sim 1$ Mev (10^{10} K), we had

$$\eta_b \equiv \frac{n_b}{n_\gamma} = 5.5 \times 10^{-10} \left(\frac{\Omega_b h^2}{0.020} \right)$$

Thus in the early universe with $T \sim 1$ MeV there were many more photons than baryons.

The mass of a proton is 938.3 MeV/ c^2 . A neutron is slightly heavier than a proton, $(m_n - m_p)c^2 = 1.3$ Mev; the difference is $\sim 0.14\%$ of the proton mass.

Neutrons and protons can interconvert via weak interactions. When only the right arrow holds the second reaction listed below is electron capture, while the third is β -decay.

$$p + \bar{\nu} \rightleftharpoons n + e^+, \quad p + e^- \rightleftharpoons n + \nu, \quad n \rightleftharpoons p + e^- + \bar{\nu}.$$

For $T > 1$ MeV (10^{10} K), the reactions listed above can proceed in both directions. Statistical equilibrium then determines the ratio between n and p ,

$$\frac{N_n}{N_p} = \left(\frac{m_n}{m_p}\right)^{3/2} \exp\left[-\frac{(m_n - m_p)c^2}{kT}\right]$$

Note that under these circumstances, **once T is specified, the ratio of neutrons to protons is determined.**

At very high T , there are no atomic nuclei, just free neutrons, protons and electrons. Any nuclei beyond p that might be formed are destroyed immediately by high energy photons. And the ratio of neutrons to protons is almost one.

As T decreases, the ratio N_n/N_p decreases, and protons outnumber neutrons. At $T \sim 0.8$ MeV, the mean time for the second reaction becomes longer than the age of the universe at that epoch, ~ 2 sec. At this time, the neutrons freezeout; no more neutrons can be created, and the neutron-proton ratio is set to $\exp[-1.3/0.8] = 0.20$. A detailed calculation finds that the fraction of neutrons at freezeout $X_n = N_n/(N_n + N_p)$ is 0.15.

Production of deuterium and other light elements begins at about $T \sim 0.07$ MeV. But free neutrons have a finite lifetime, only 15 min. By the time the reactions to make nuclei are at their peak, only 74% of the neutrons are left, the remainder having become protons via β -decay.

Because of the low binding energy of the isotopes after ${}^4\text{He}$ (see the appended figure), only elements up to He and slightly beyond can be produced. Lets consider deuterium first. We are looking at the equilibrium of the reaction $n + p \rightleftharpoons D + \gamma$. Nuclear statistical equilibrium (the equivalent of the Saha equation for ionization equilibrium between various ions of a specific atom) requires

$$\frac{N_d}{N_n N_p} = \frac{3}{4} \left(\frac{2\pi m_D}{m_n m_p T}\right)^{3/2} e^{[m_n + m_p - m_d]c^2/kT} \approx \frac{3}{4} \left(\frac{4\pi}{m_p T}\right)^{3/2} e^{B_D/T},$$

where B_D is the binding energy of deuterium. Since $\eta \propto T^3/N_b$, this in turn becomes

(approximately)

$$\frac{N_d}{N_b} \propto \eta_b \left(\frac{T}{m_p}\right)^{3/2} e^{B_D/T}.$$

The exponential factor increases rapidly as T becomes less than B_D , but η , which is (n_b/n_γ) , is a very small number as shown above. The binding energy for deuterium is 2.2 MeV. But the small baryon fraction (very small η) inhibits the production of nuclei such as D or He until the temperature drops well below the nuclear binding energy, which is where one would naively think nuclear reactions would begin.

The equilibrium deuterium abundance (ignoring He) is when all the neutrons are in deuterium, and the rest of the protons are free ^1H nuclei without any electrons. To find it, all we need to know is the value of T ; given that we can find N_p/N_n and hence the deuterium fraction.

But the binding energy of He is much larger than for deuterium, so very little deuterium gets produced; almost all of the neutrons go into ^4He nuclei, each of which requires 2 neutrons.

Some neutrons β -decay into $+e^- + \bar{\nu}$ before making it into a He nucleus, and a very small fraction end up in isotopes other than ^4He , i.e. ^2H , ^3He , Li and Be. That plus the delay from the high photon/baryon density reducing T_{nuc} changes N_n/N_p from about 1/5 to 1/7. The predicted ratio of $^4\text{He}/\text{H}$ is then 1/12 (i.e. for every ^4He nucleus, there are 12 free protons). The mass fraction of He is then predicted to be $4/(12 + 4) = 1/4$, which is extremely close to that observed. Obviously this argument can be worked out in detail to predict the $^4\text{He}/\text{H}$ more carefully.

We expect that $X_4 = 4 \times n(^4\text{He})/n_b = 2X_n(T_{nuc})$, and the crucial thing is establishing the appropriate T_{nuc} . Using the the value of T_{nuc} we found from the D/H ratio, we then

find a He mass fraction from Big Bang nucleosynthesis of $Y_p = 0.22$. Observations from HII regions, where emission lines of both He and H can be detected, extrapolated to zero metallicity, suggest $Y_p = 0.238$, in good agreement with this rather crude prediction.

A more careful detailed treatment yields ratios of D/H (10^{-5}), ${}^3\text{He}/\text{H}$ (10^{-5}), ${}^7\text{Li}/\text{H}$ (10^{-9}), and almost nothing else. Clearly H and ${}^4\text{He}$ dominate. These predictions depend on the baryon density at the time of neutron freezeout, n_b .

Measurements of the CMB photon density today can be used to infer η . The CMB fluctuation spectrum also depends on the baryon density, and observations give a consistent value of n_b today, usually expressed as a fraction of the critical closure density. This precision measurement of the value of η can be compared to the value required for the predicted primordial abundances of the elements and their isotopes listed above to agree with those observed in the most metal-poor stars, extrapolated to zero metallicity.

The WMAP measurement of baryon/photon ratio η is $6.23 \pm 0.17 \times 10^{-10}$ (Cyburt et al 2008). We stress that this **determines** the primordial abundances of the stable isotopes of He, Li, Be and B, with the predicted value of $\log[{}^7\text{Li}/\text{H}] = 2.72 \pm 0.06$ dex. (Here the conventional notation is used, abundances are calculated with respect $n(H)$ set to 10^{12} and are given as logs in base 10, so the above converts to $n(\text{Li})/n(H) = 5 \times 10^{-10}$.) One must assume for these calculations a value for the number of flavors of neutrinos; almost all calculations adopt that as three.

Agreement between the observed and predicted big bang nucleosynthesis for the isotopes of He and the lightest elements is a key test of big bang cosmology. The element of choice for this test is the D/H ratio, as D is only destroyed in stars. So $(\text{D}/\text{H})(\text{obs}) \leq (\text{D}/\text{H})(\text{big bang})$, and in stars of very low metallicity, the observed value should approach the primordial value.

D/H is hard to measure. The usual technique is to look at absorption lines in the spectra of distant QSOs arising from intervening gas. See papers by David Tytler or Max Pettini. Pettini's 2006 conference presentation (astro-ph/0601428) is a good review of the situation. The mean is about $\log[\epsilon(\text{D})] = 0.45$, i.e. $D/H = 2.8 \times 10^{-11}$. Adopting the value of η which produces this D/H ratio using standard BBN, ${}^3\text{He}/\text{H}$ is then 1.8×10^{-11} , $\log[\epsilon(\text{Li})] = 2.67 \pm 0.07$, etc.

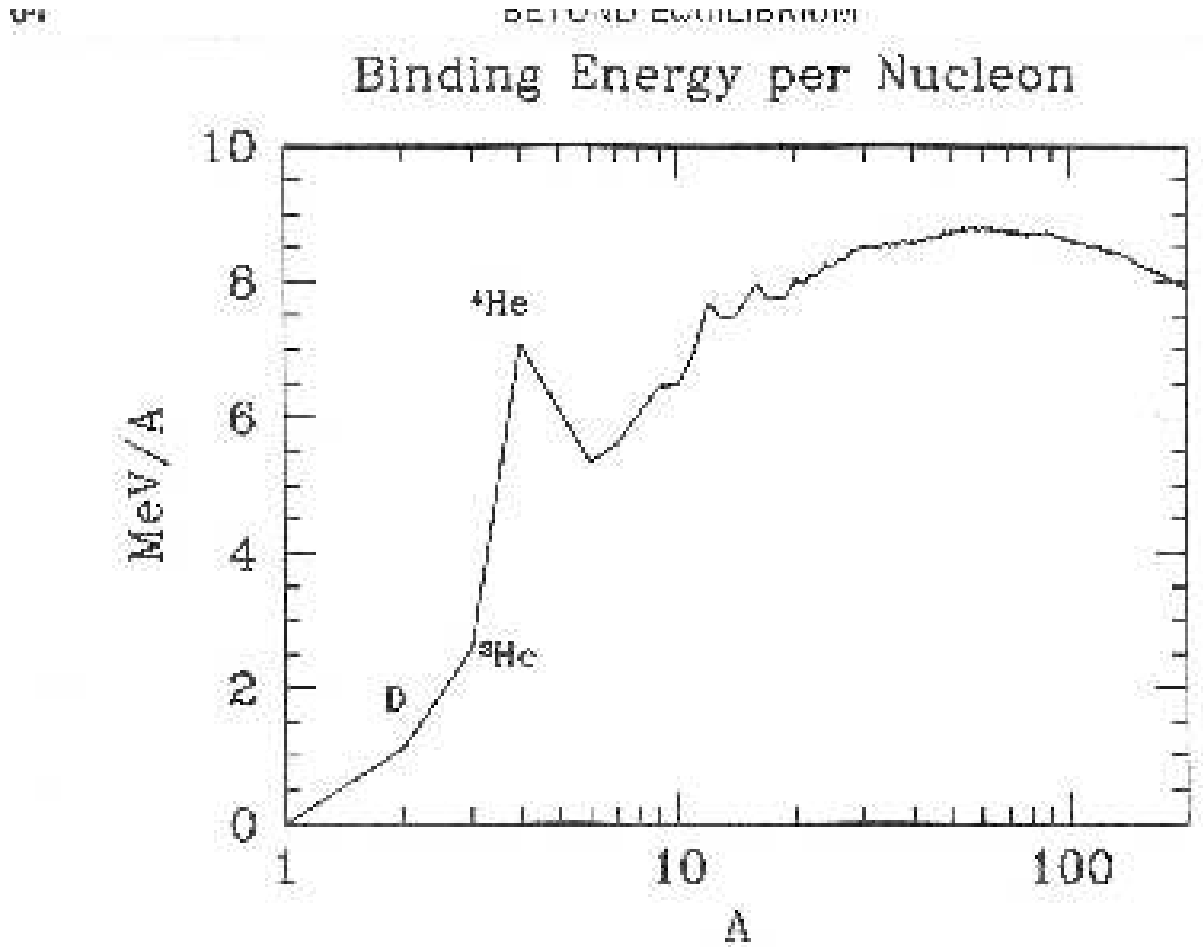


Fig. 1.— Binding energy per nucleon of nuclei as a function of mass number. Iron has the highest binding energy, but among the light elements, ${}^4\text{He}$ is a crucial local maximum. Nucleosynthesis in the early universe essentially stops at ${}^4\text{He}$ because of the lack of tightly bound isotopes with atomic mass between 5 and 8. In the centers of stars, 3 ${}^4\text{He}$ nuclei fuse to form ${}^{12}\text{C}$, but the density in the early universe is too low for this process to operate there. (Fig. 3-1 of Dodolson, *Modern Cosmology*)

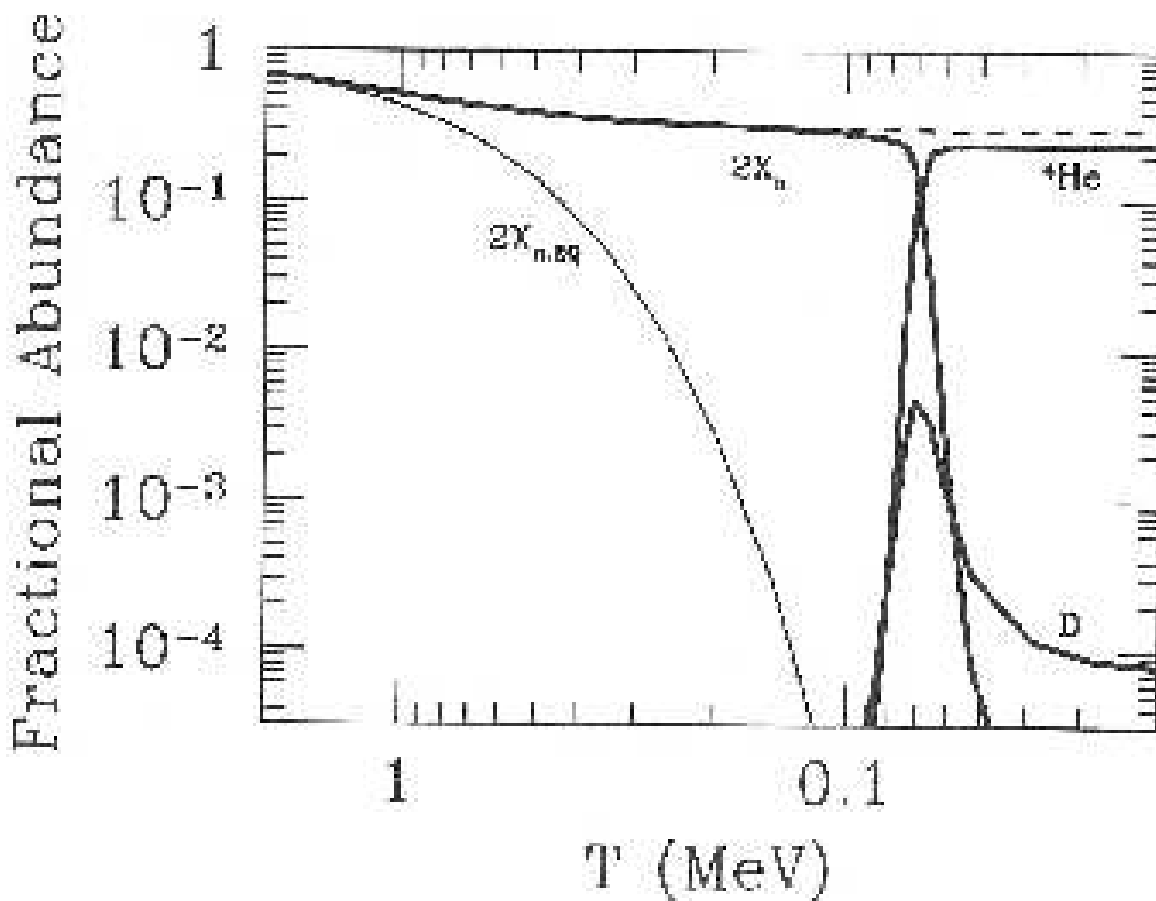


Fig. 2.— Evolution of light elements in the early universe. The heavy solid curves are from a detailed numerical solution to the full set of equations, the dashed curve is from a simple integration of the nuclear statistical equilibrium equation (the “Saha” equation for nuclei). These two agree extremely well until the onset of neutron decay. The light solid curve is simply $2 \times X_n$ from nuclear statistical equilibrium at each temperature. The neutrons fall out of equilibrium at $T \sim 1$ MeV, as expected from the mass difference between protons and neutrons. (Fig. 3-2 of Dodolson, *Modern Cosmology*)

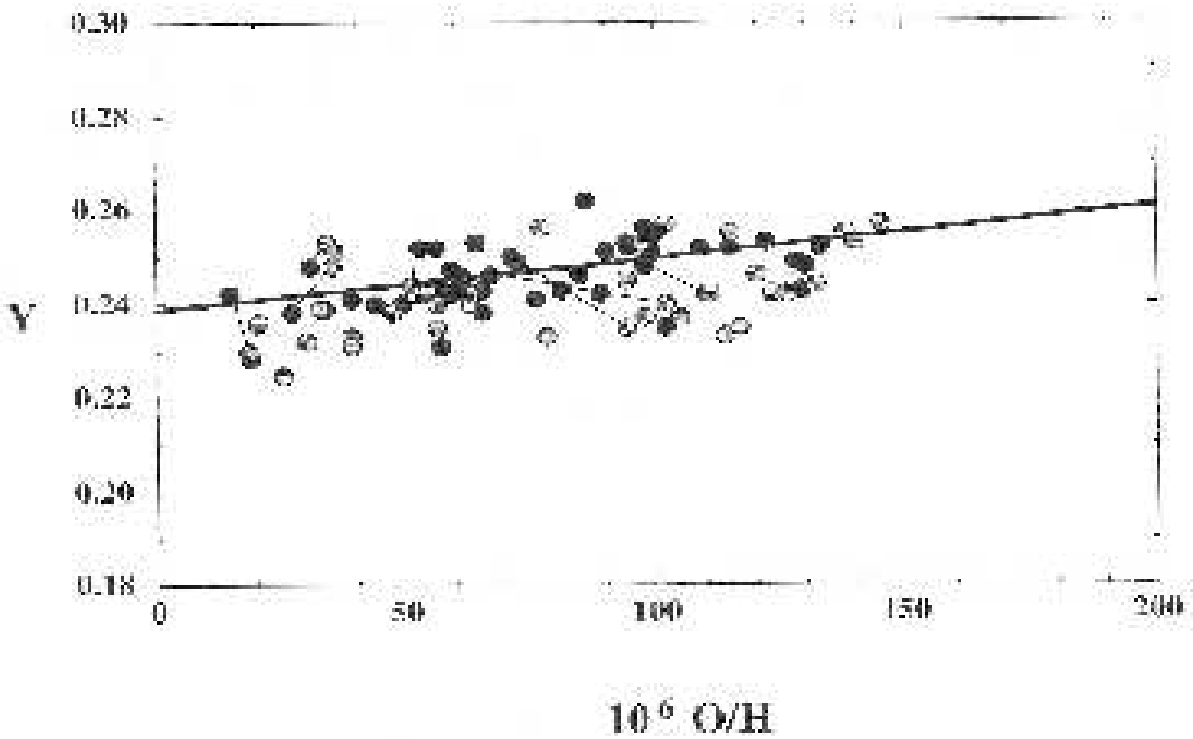


Fig. 3.— The He abundance by mass Y as a function of the oxygen to hydrogen ratio. These are a compilation of analyses of the emission line spectra of HII regions, where lines of H, He, and O are fairly easy to detect. Oxygen is used as a proxy for nuclear processing (instead of Fe, usually the element of choice for stars). Lower oxygen systems have had less stellar processing and presumably have He closer to the primordial value. The fit line, when extrapolated to no oxygen, measures $Y_p = 0.238$. (Fig. 3-3 of Dodolson, *Modern Cosmology*)

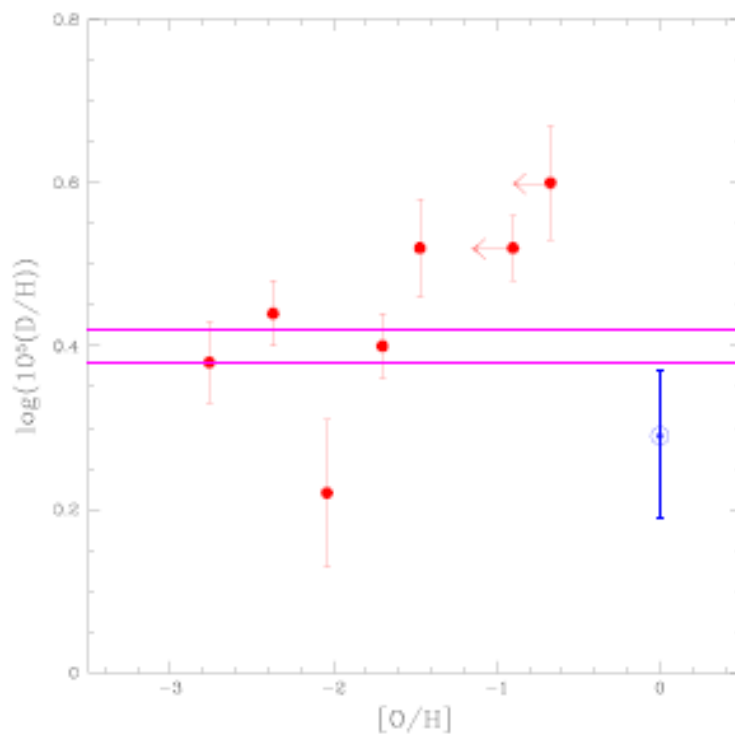


Figure 1. The logs of the deuterium abundances, $\nu_D \equiv 10^5(D/H)$, observed in high- z , low- Z QSO Absorption Line Systems (Pettini *et al.* (2008)), as a function of the corresponding oxygen abundances. For comparison, the solar deuterium and oxygen abundances are shown (Geiss & Gloeckler (1998)). The band indicated by the solid lines is the 68% range of the SBBN-predicted primordial D abundance using the CMB-determined baryon density parameter (see §3).

Fig. 4.— Fig. 1 of G. Steigman, from IAU Symposium 268, 2010, see arXiv:0912.1114

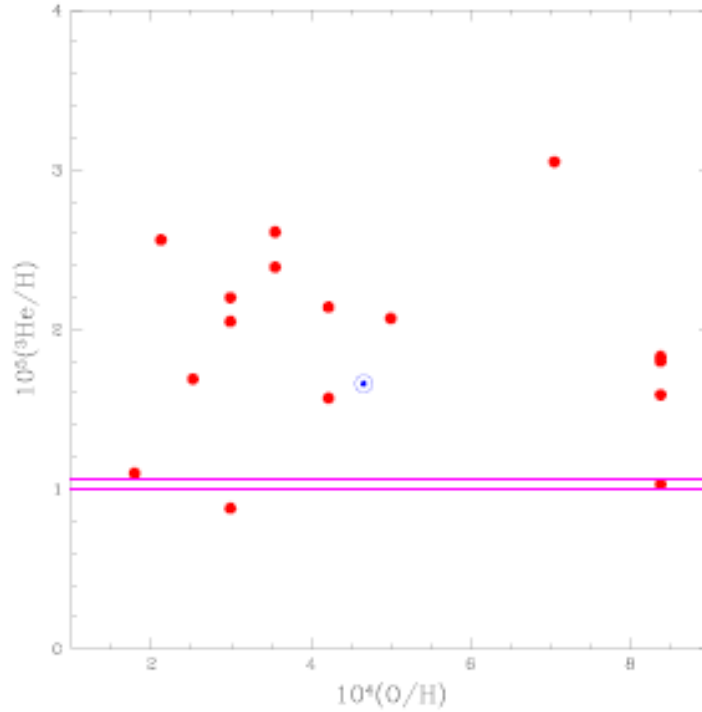


Figure 2. The ^3He abundances, $y_3 \equiv 10^5(^3\text{He}/H)$, observed in Galactic H II regions from [Bania, Rood, & Balser \(2002\)](#) are shown as a function of the corresponding oxygen abundances. For comparison, the solar helium-3 and oxygen abundances are shown. The band indicated by the solid lines is the 68% range of the SBBN prediction for the primordial ^3He abundance using the CMB-determined baryon density parameter (see §3).

Fig. 5.— The same as the previous figure, but for ^3He . Fig. 2 of G. Steigman, from IAU Symposium 268, 2010, see arXiv:0912.1114

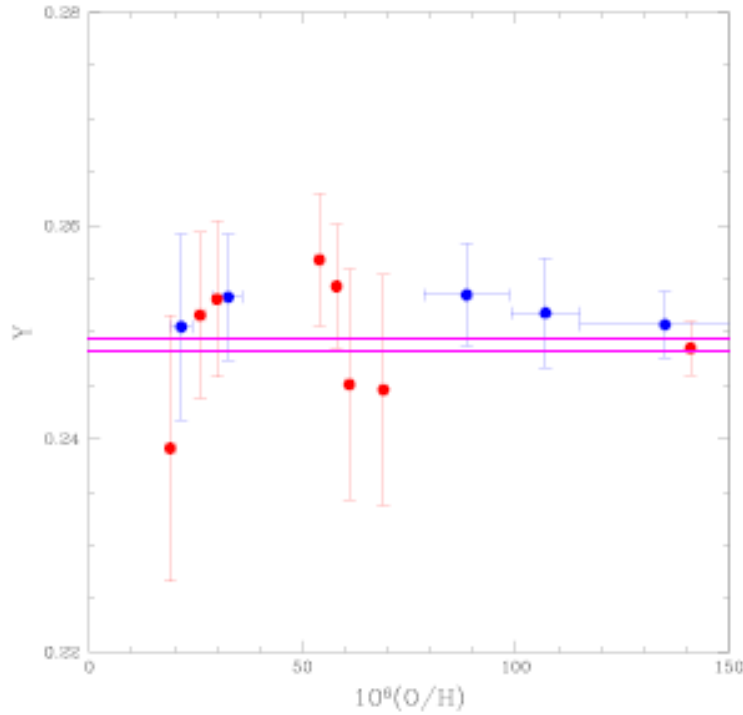


Figure 3. The ^4He mass fractions, Y , derived from a selected sample (see the text) of low metallicity, extragalactic HII regions, as a function of the corresponding HII region oxygen abundances. The blue filled circles are from Peimbert, Luridiana, & Peimbert (2007) and the red filled squares are from Olive & Skillman (2004). The band indicated by the solid lines is the 68% range of the SBBN prediction for the primordial ^4He mass fraction using the CMB-determined baryon density parameter (see §3).

Fig. 6.— The same as the previous figure, but for ^4He . Fig. 3 of G. Steigman, from IAU Symposium 268, 2010, see arXiv:0912.1114

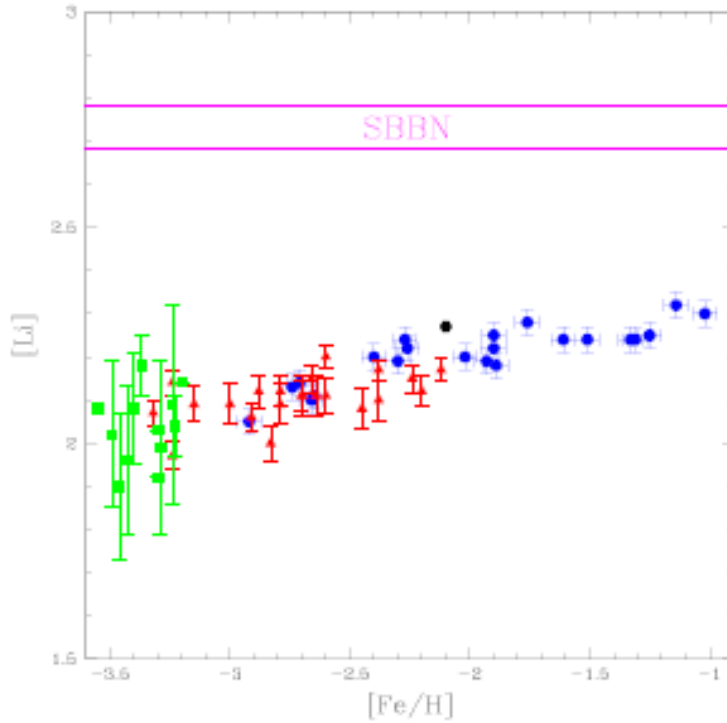


Figure 4. The lithium abundances, $[Li] \equiv 12 + \log(Li/H)$, derived from observations of low metallicity Galactic halo and globular cluster stars as a function of the iron abundance (relative to solar). Blue filled circles (Asplund *et al.* (2006)), red, filled triangles (Boesgaard *et al.* (2005)), green filled squares (Aoki *et al.* (2009)). The black filled circle (Lind *et al.* (2009)) is for the globular cluster NGC6397. The band indicated by the solid lines is the 68% range of the SBBN prediction for the primordial ${}^7\text{Li}$ abundance using the CMB-determined baryon density parameter (see §3).

Fig. 7.— The same as the previous figure, but for Li. Fig. 4 of G. Steigman, from IAU Symposium 268, 2010, see arXiv:0912.1114

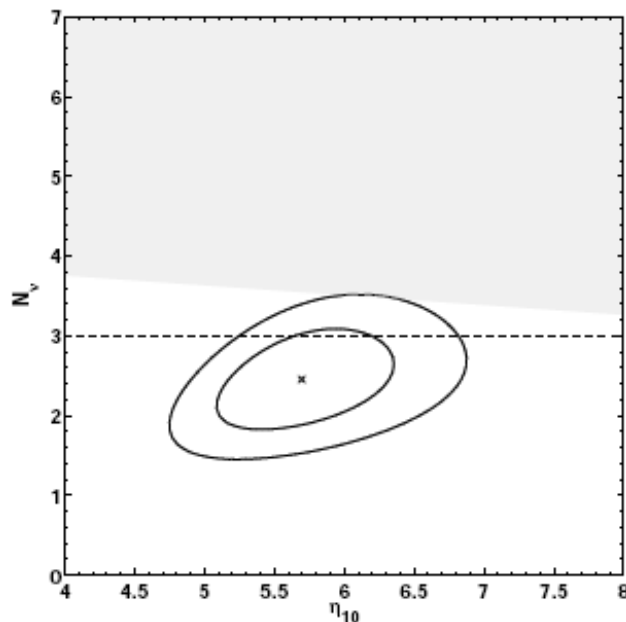


Figure 2:

The 68% and 95% contours in the $N_\nu - \eta_{10}$ plane inferred from BBN using the D and ${}^4\text{He}$ abundances adopted in §2.1 and §2.3 respectively. The “x” marks the “best fit” point^[2] at $\eta_{10} = 5.7$ and $N_\nu = 2.4$. The shaded area corresponds to the combination of N_ν and η_{10} leading to a BBN-predicted ${}^4\text{He}$ mass fraction in excess of the observationally-inferred upper bound of 0.255; see §2.3.

Fig. 8.— The shaded area referred to in the caption of this figure is the upper half of the figure just above the indicated two contours, with its bottom edge sloping slightly lower to the right side of the figure. This is Fig. 2 from the contribution of G. Steigman to the International Workshop on Neutrino Oscillations, 2008, see arXiv:0807.3004.

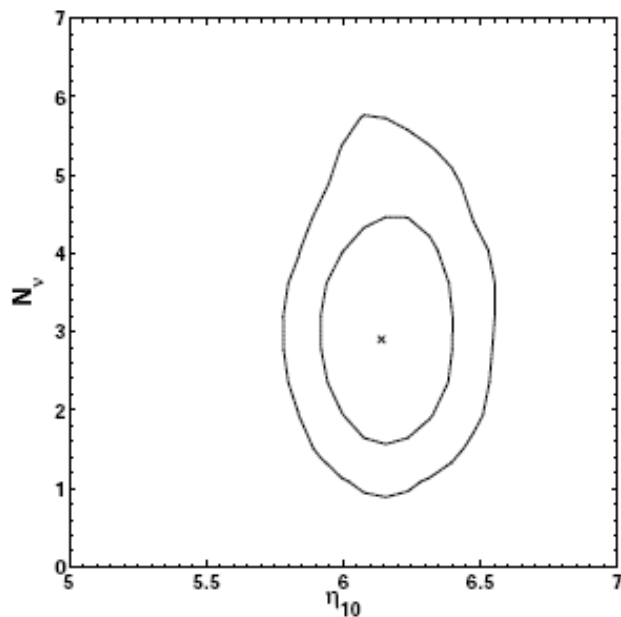


Figure 3:

The 68% and 95% contours in the $N_\nu - \eta_{10}$ plane derived using the WMAP 5-year data, small scale CMB and SNIa data, and the HST Key Project prior on H_0 along with data from the LSS matter power spectrum (see the text).

Fig. 9.— Fig. 3 of G. Steigman, from the International Workshop on Neutrino Oscillations, 2008, see arXiv:0807.3004. see arXiv:0912.1114

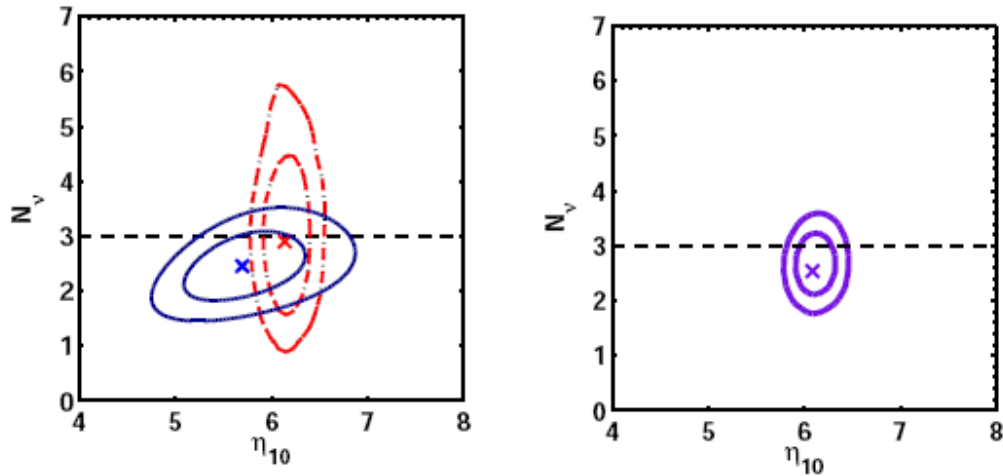


Figure 4:

(Left) In blue (solid), the 68% and 95% contours in the $N_\nu - \eta_{10}$ plane derived from a comparison of the observationally-inferred and BBN-predicted primordial abundances of D and ^4He . In red (dashed), the 68% and 95% contours derived from the combined WMAP 5-year data, small scale CMB data, SNIa, and the HST Key Project prior on H_0 along with the LSS matter power spectrum data. (Right) The 68% and 95% joint BBN-CMB-LSS contours in the $N_\nu - \eta_{10}$ plane.

Fig. 10.— Fig. 4 of G. Steigman, from the International Workshop on Neutrino Oscillations, 2008, see arXiv:0807.3004. see arXiv:0912.1114

1.1. Li, Be, and B

Li, Be, and B (henceforth denoted L) are very fragile elements (as is the heavy isotope of H, deuterium), and are destroyed in stars for $T > 2 \times 10^6$ K. Thus although L may be produced in nuclear reactions in the stellar core, they will immediately be destroyed.

Both isotopes of Li are produced in the Big Bang, but at a very low abundance. ${}^7\text{Li}$ is also produced in AGB stars and in novae, but these do not contribute to the chemical inventory of the most metal-poor stars.

Most of Li, and essentially all of Be and B are nuclear spallation products resulting from collisions of primary energetic protons and α -particles (He nuclei) (as cosmic rays) with C, N, and O in the interstellar medium leading to fragmentation (spallation). To model this, one needs to model the variation with time of the CNO abundances in the ISM of the Milky Way, the flux of primary cosmic ray protons, $\phi(t)$, and of α particles (${}^4\text{He}$ nuclei stripped of their electrons), the energy spectra for the protons and α particles, and the production cross sections as a function of energy. Since $d(L/H)/dt \propto z(t)\sigma\phi(t)$, we find $(L/H) \propto z(t)^2$, the classic equation for the evolution of a secondary element.

This does not match the observational data for Be/H or B/H vs [Fe/H]. Assuming the oxygen abundance \propto Fe/H, another production mechanism must be contributing. This is hypothesized to be lower energy CO nuclei produced in hot massive stars, ejected by their winds at high velocity into cavities in the ISM created by such high luminosity stars, fragmenting on H and He at rest in the ISM. Li, Be, and B would then be primary nuclei, whose abundances increased linearly with z , instead of quadratically. Probably the truth is a mixture of both primary cosmic ray and massive star spallation, with the latter dominating at low metallicity, then the cosmic ray contribution dominating above that.

There is currently a controversy about the value of the ${}^6\text{Li}/{}^7\text{Li}$ ratio and also the

abundance of Li in metal-poor stars vs that predicted by primordial nucleosynthesis just after the Big Bang. Using the WMAP measurement of baryon/photon ratio η , the primordial abundance of $\log[\epsilon(^7\text{Li})]$ is 2.72 ± 0.06 dex. But the observed Li abundance in extremely metal poor stars is between 2.0 and 2.3 dex, and no one has been able to push it higher by a factor of 2.5 so as to reach 2.7 dex. However, there are some concerns with the stellar values, so it is premature to claim disagreement with Big Bang nucleosynthesis. Early astration, diffusion, the very strong T dependence of the total Li abundance may all be contributing.

With regard to the Li isotope ratio, Asplund, Lambert, Nissen, Primas & Smith (2006, ApJ, 644, 229) claimed to detect ^6Li in metal-poor stars at the level of a few percent of the total Li. Such a high ^6Li abundance is very difficult to achieve from cosmic ray spallation early in the history of the galaxy, and is also far above that which is expected from big bang nucleosynthesis. The latter is well constrained because we know η , the ratio of baryons to protons from the CMB, and we can thus do accurate calculations of big bang nucleosynthesis successfully for ^4He and ^2H (deuterium). Such calculations predict $^6\text{Li}/^7\text{Li} \sim 10^{-5}$, far lower than the ratios claimed by Asplund and collaborators.

This is an extremely difficult measurement. The claimed ^6Li fraction is only a few percent, so it must be detected as a small blip in the red wing of the ^7Li 6707 Å feature, which is itself a doublet. Extremely accurate profiles for this key Li line are required, as well as careful modeling. See Steffen, Cayrel, Bonifacio, Ludwig & Caffau (2010, Proc. IAU Symposium 268, 2010, or arXiv:1001.3274) and papers referenced therein for a discussion of the relevant issues.

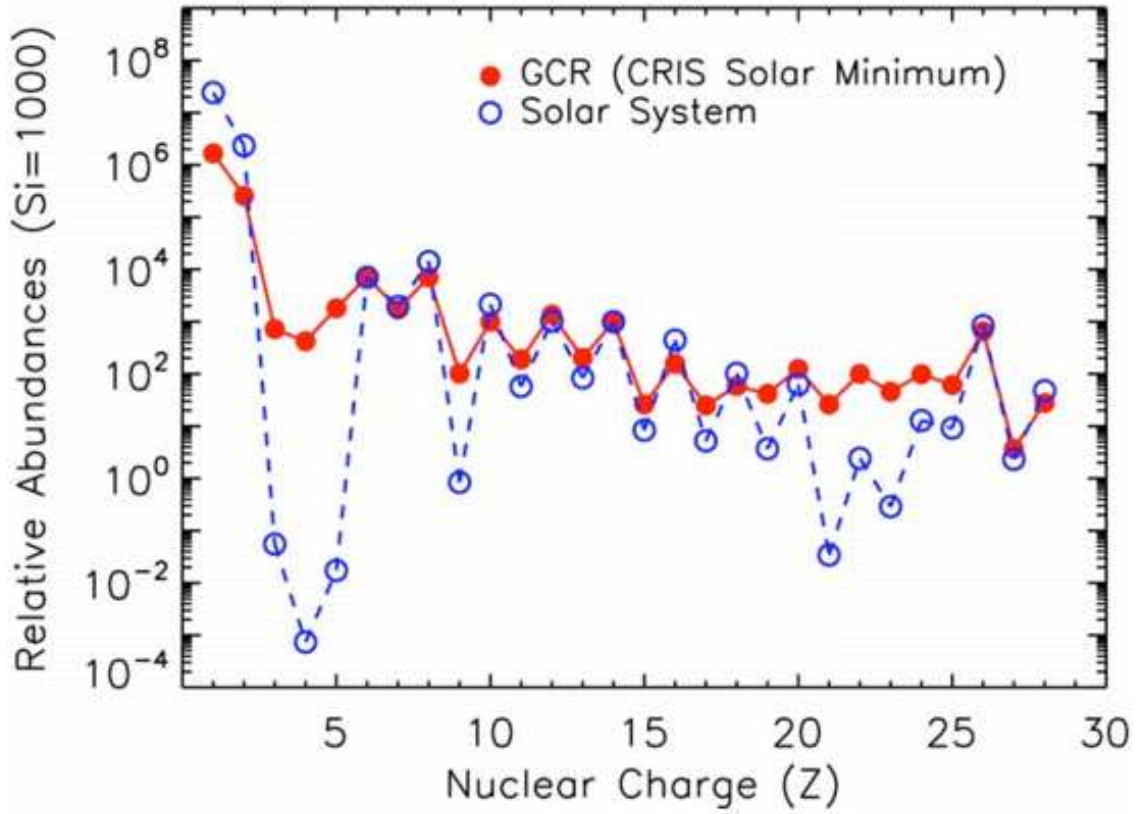


Fig. 11.— Fig. 7 of George, Lave, Wiedenbeck et al, 2009, ApJ, 698, 1666, based mostly on ACE data. The typical energy is ~ 200 MeV/nuc near the peak in the spectrum at 1 AU.

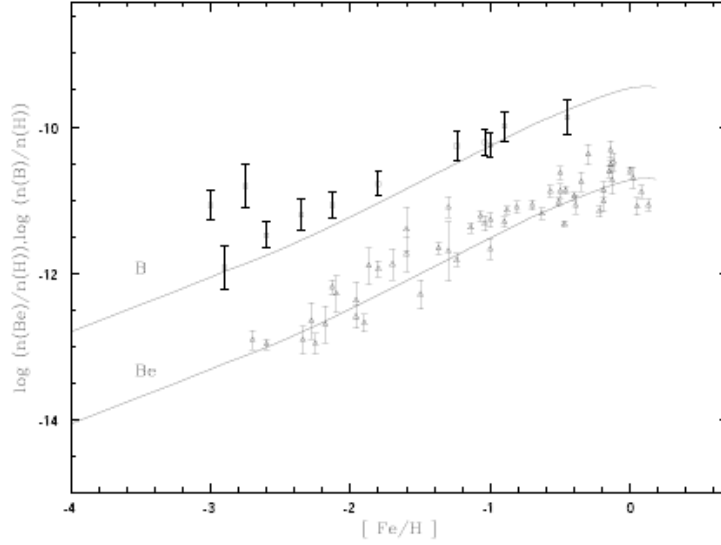


Fig. 1. Beryllium and Boron evolution vs $[Fe/H]$. The halo evolution is dominated by the LEC component (primary) emanating from supernovae. The contribution of the standard GCR component (secondary) is insignificant below $[Fe/H] < -1$ if O is proportional to Fe, if not, i.e. $[O/Fe] \propto [Fe/H]$, the transition between primary and secondary processes could occur around $[Fe/H] = -2$, Vangioni-Flam et al 1998, Fields and Olive 1999.

Fig. 12.— Fig. 1 from Vangioni-Flam & Casse, 2001, review for IAU Symposium, see astro-ph/0104194. The horizontal axis is iron metallicity, $[Fe/H]$. The vertical axis is $\log[\epsilon(\text{Be or B})]$. The curve for Be lies below that for B.

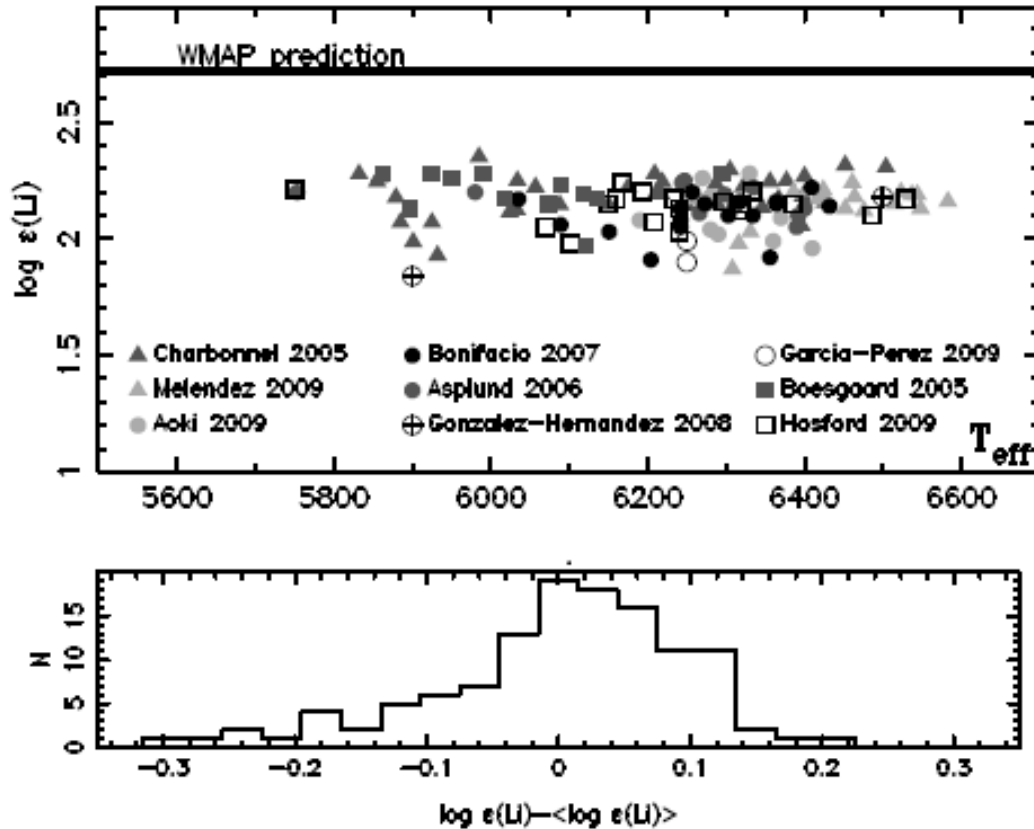


Figure 1. Lithium abundance versus Temperature for metal-poor stars ($[\text{Fe}/\text{H}] < -2$) and (below) histogram. Triangles indicate that the temperature has been determined from photometry, circles from the profile of the hydrogen lines and squares from the excitation temperature. In this interval of temperature and metallicity, the lithium abundance is independent of the temperature but the scatter is rather large. The mean value of the lithium abundance is $\log \epsilon(\text{Li}) \approx 2.15$, more than 0.55 dex below the prediction of standard BB + WMAP (full black line). On the histogram showing the distribution of the distances of each point to the mean value of the lithium abundance it can be seen that the distribution is not gaussian.

Fig. 13.— Fig. 1 from Spite & Spite (2010) (IAU Symposium 268), see arXiv:1002.1004.

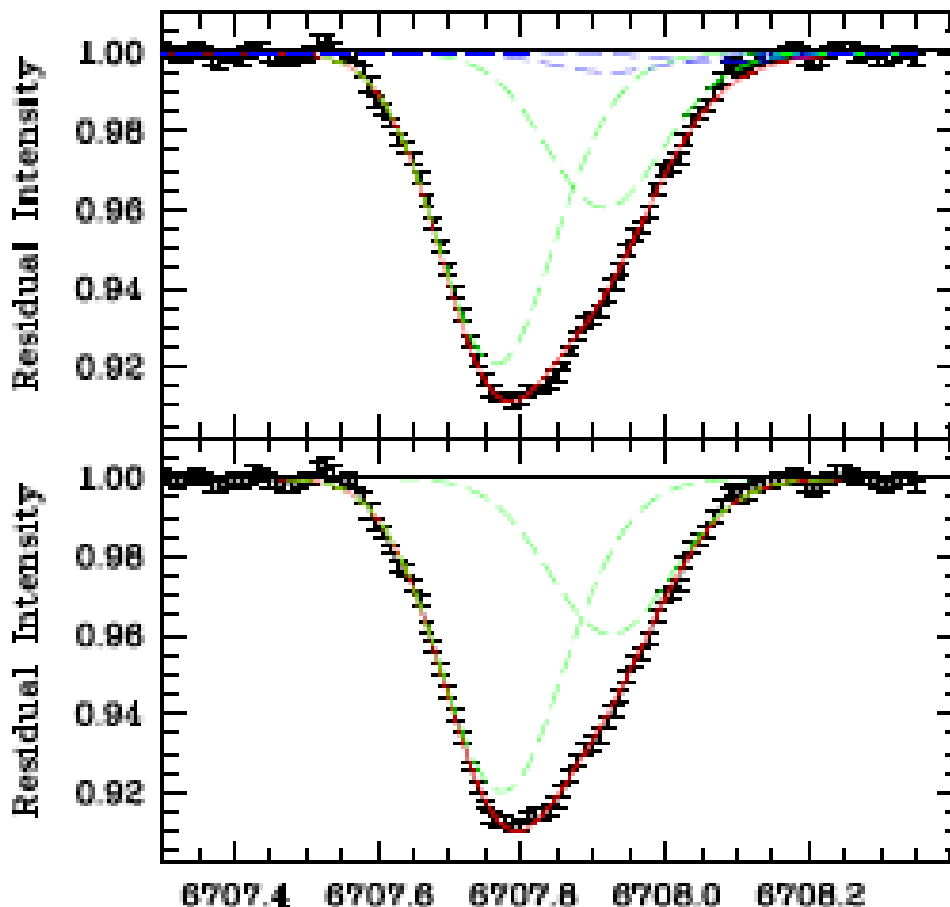


Fig. 3. Upper panel: The observed Li doublet (black dots with error bars), together with the best fitting synthetic profile (red solid line) computed using the empirical profile derived from the Fe I lines. The green dashed lines show the ${}^7\text{Li}$ components and the blue dashed lines the ${}^6\text{Li}$ components. Fitting parameters are the contributions of ${}^7\text{Li}$ and ${}^6\text{Li}$ and thermal broadening, but no global wavelength shift was allowed. See text for details. Lower panel: like upper panel, but also allowing for a global wavelength shift, the best fit corresponds to a shift of 372 m s^{-1} .

Fig. 14.— Fig. 3 from Cayrel, Steffen, Chand, et al (2007, A&A, 473, L37) illustrating the extreme difficulty of detecting a small contribution of ${}^6\text{Li}$ to the profile of the 6707 Å Li doublet.

2. Topics for Student Discussion

1. Li abundance and isotope ratio in extremely metal poor stars vs Big Bang nucleosynthesis.
2. Discuss the D/H measurements from QSO absorption lines and the uncertainties in these measurements. What can go wrong ?